

AN UNBIASED CENSUS OF ACTIVE GALACTIC NUCLEI IN THE TWO MICRON ALL SKY SURVEY

PAUL J. FRANCIS¹

Research School of Astronomy and Astrophysics, Australian National University, Canberra, ACT 0200, Australia; pfrancis@mso.anu.edu.au

AND

BRANT O. NELSON AND ROC M. CUTRI

Infrared Processing and Analysis Center, Mail Code 100-22, California Institute of Technology, 770 South Wilson Avenue,
Pasadena, CA 91125; nelson@ipac.caltech.edu, roc@ipac.caltech.edu

Received 2003 June 11; accepted 2003 October 16

ABSTRACT

We present an unbiased near-IR-selected AGN sample, covering 12.56 deg^2 down to $K_s \sim 15.5$, selected from the Two Micron All Sky Survey (2MASS). Our only selection effect is a moderate color cut ($J - K_s > 1.2$) designed to reduce contamination from Galactic stars. We observed both pointlike and extended sources. Using the brute-force capabilities of the Two Degree Field multifiber spectrograph on the Anglo-Australian Telescope, we obtained spectra of 65% of the target list: an unbiased subsample of 1526 sources. Eighty percent of the 2MASS sources in our fields are galaxies, with a median redshift of 0.15. The remainder are K and M dwarf stars. We find tentative evidence that Seyfert 2 nuclei are more common in our IR-selected survey than in blue-selected galaxy surveys. We estimate that $5.1 \pm 0.7\%$ of the galaxies have Seyfert 2 nuclei with $H\alpha$ equivalent widths greater than 0.4 nm, measured over a spectroscopic aperture of radius ~ 2.5 kpc. Blue-selected galaxy samples only find Seyfert 2 nuclei meeting these criteria in $\sim 1.5\%$ of galaxies. We find that $1.2 \pm 0.3\%$ of our sources are broadline (type 1) AGNs, giving a surface density of $1.0 \pm 0.3 \text{ deg}^2$, down to $K_s < 15.0$. This is the same surface density of type 1 AGNs as optical samples down to $B < 18.5$. Our type 1 AGNs, however, mostly lie at low redshifts, and host galaxy light contamination would make $\sim 50\%$ of them hard to find in optical QSO samples. We conclude that the type 1 AGN population found in the near-IR is not dramatically different from that found in optical samples. There is no evidence for a large population of AGNs that could not be found at optical wavelengths, although we can only place very weak constraints on any population of dusty high-redshift QSOs. In contrast, the incidence of type 2 (narrow-line) AGNs in a near-IR-selected galaxy sample seems to be higher than in a blue-selected galaxy sample.

Key words: galaxies: active — quasars: general — surveys

On-line material: machine-readable table

1. INTRODUCTION

To date, nearly all complete active galactic nucleus (AGN) samples are flux-limited at blue optical wavelengths. Such surveys are highly efficient and can be very complete (e.g., Meyer et al. 2001), picking up all AGNs *down to their blue flux limit*. Unfortunately, any survey with a blue flux limit will be relatively insensitive to objects whose emission peaks at any other wavelength.

How seriously does this blue flux limit bias AGN samples? The situation is somewhat different for QSO searches (searches for AGNs which are considerably brighter than their host galaxy) and Seyfert galaxy searches (searches for less luminous AGNs).

1.1. Luminous QSOs

There has long been speculation that there might exist a substantial population of luminous QSOs with red colors in the optical/near-IR. These red colors could be caused by small quantities of dust, or the QSOs could be intrinsically red. Given the steepness of the luminosity function for luminous QSOs, most will lie close to the magnitude limit of a survey,

so even small amounts of extinction will eliminate them from a blue-selected sample (Fig. 1).

QSOs live in the nuclei of galaxies, which are dusty places. It should, therefore, be no surprise that our sight line to the centers of many QSOs is obscured by dust. What is surprising is that the dust seems to either completely obscure our view of the central engine of the QSO (type 2 AGN) or not to obscure it at all (type 1 AGN). There seem to be very few QSOs that are partially obscured by dust, so that we still see a nuclear QSO spectrum, albeit a reddened one. Our sight line seems either to intersect a giant molecular cloud or no dust at all. This contrasts with sight lines from the Earth out of our Galaxy, most of which intersect small quantities of optically thin dust (Schlegel, Finkbeiner, & Davis 1998). Is this a selection effect, or does AGN activity expel or destroy optically thin dust, as suggested by Dopita et al. (1998)?

A few red QSOs have now been found. Many radio-selected quasars are quite red, although this redness may be caused by synchrotron emission or weak blue bump emission, rather than dust (Webster et al. 1995; Baker & Hunstead 1995; Whiting, Webster, & Francis 2001; Francis, Whiting, & Webster 2000; Francis et al. 2001). At least a few radio-selected quasars, however, show unmistakable evidence of severe dust reddening (Malhotra, Rhoads, & Turner 1997; Courbin et al. 1998; Gregg et al. 2002). A handful of red AGNs have also been

¹ Joint appointment with the Department of Physics, Faculty of Science, Australian National University.

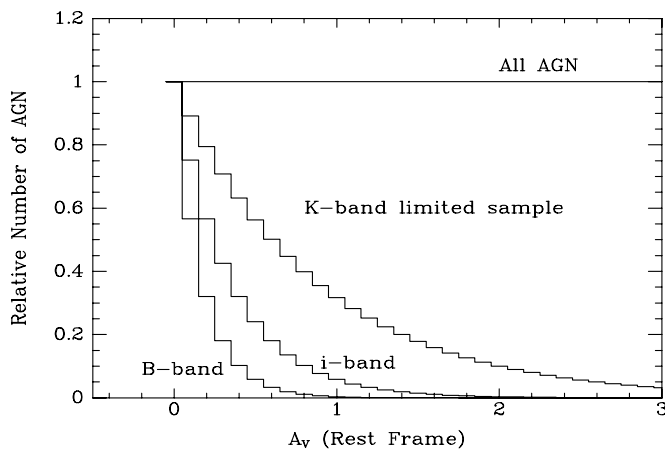


FIG. 1.—Predicted numbers of QSOs found as a function of dust extinction. The model assumes that the real population of QSOs is uniformly distributed per unit dust extinction A_V , where A_V is the absorption in the rest-frame V -band in magnitudes (the QSOs are assumed to lie at redshift 1). The labeled curves show the fraction of these QSOs that would be found in complete surveys, magnitude-limited in the B , i , and K_s bands. A luminosity function appropriate for bright QSO samples has been assumed. Dust is assumed to have an optical depth inversely proportional to wavelength and to lie at the QSO redshift.

identified in other surveys (e.g., McDowell et al. 1989; Brotherton et al. 2001).

To accurately determine the population of red QSOs and to better characterize their apparently diverse nature, a QSO sample with a magnitude limit at some wavelength unaffected by dust would be ideal. Radio surveys only pick up the small fraction of QSOs that are radio-loud, which are probably not representative. Hard X-ray surveys (e.g., Mushotzky et al. 2000; Alexander et al. 2001) are unaffected by dust, but many hard X-ray sources are so faint at optical wavelength that follow-up spectroscopy is very difficult, even with large telescopes. It does, however, seem clear that dusty AGNs are a major contributor to the X-ray background. Far-IR selection (e.g., Low et al. 1988; Matute et al. 2002) is biased toward dusty sources, but discriminating between QSOs and starburst galaxies has proven extremely hard.

Complete near-IR-selected surveys are still somewhat biased against dusty QSOs (Fig. 1). They have the major advantage that most QSOs found in a near-IR-limited survey will be bright enough for relatively easy follow-up spectroscopy. Surveys with i -band magnitude limits, such as the Sloan Digital Sky Survey (SDSS) QSO survey (Richards et al. 2002), are an improvement on B -band-limited surveys, but Figure 1 makes it clear that going still further to the red should yield big gains.

Can we construct a complete K -band-limited QSO sample? Warren, Hewett, & Foltz (2000) showed that by combining optical and near-IR photometry, it should be possible to construct such a sample. Unfortunately, suitable photometry does not yet exist over larger areas of the sky, although the technique has been successfully applied in one small region (Croom, Warren, & Glazebrook 2001).

1.2. Seyfert Nuclei

The situation is somewhat different for less luminous AGNs. These cannot be found by color selection, as the host galaxy light dominates their broadband colors. They are normally found by getting spectra of the nuclear regions of large samples of galaxies (e.g., Huchra & Burg 1992; Ho, Filippenko, &

Sargent 1997). To date, these galaxy samples have been magnitude-limited in the blue. This may well introduce a bias: the blue light from galaxies is dominated by young stars and is hence an indication of recent star formation.

The near-IR light from galaxies is coming from an older stellar population and hence correlates with the total stellar mass rather than the recent star formation rate. Near-IR-selected galaxy samples are dominated by elliptical galaxies, unlike blue-selected samples which are dominated by spirals.

We might thus expect the population of AGNs in an IR-selected galaxy sample to differ from that in a blue-selected sample for many reasons. The black hole masses, which are known to correlate with the bulge stellar mass, should be larger. If accretion onto the black hole correlates with star formation, we might be looking at lower accretion rates. Dust properties may be quite different, altering the ratios of obscured (type 2) and unobscured (type 1) AGNs.

1.3. Searching for AGNs in 2MASS

By far the largest near-IR survey to date is the Two Micron All Sky Survey (2MASS; Skrutskie et al. 1997). There have already been several studies of the different AGN populations within 2MASS. Cutri et al. (2002) have shown that 2MASS sources with extremely red near-IR colors ($J-K_s > 2$) are mostly an unusual type of type 1 AGN (Smith et al. 2002; Wilkes et al. 2002). K_s is a filter similar to K but cutting off at a shorter red wavelength to minimize thermal emission (Skrutskie et al. 1997). Barkhouse & Hall (2001) have studied the 2MASS colors of QSOs identified at other wavelengths, and Gregg et al. (2002) identified some very unusual and dusty QSOs by cross-correlating the 2MASS database with a radio sample. While these various papers clearly show that 2MASS imaged large numbers of AGNs, none of them made any pretense at giving an unbiased picture of the AGN population within 2MASS.

In this paper, we assemble a relatively unbiased sample of 2MASS AGNs. We use brute force: we apply only a very weak color selection and then use multiobject spectroscopy to pick out the few AGNs from the large contamination of other objects.

Our only selection criteria were that an object had to be detected in all three 2MASS bands and that it had $J-K_s > 1.2$. This color cut was designed to eliminate halo giant and disk dwarf stars (the peaks at $J-K_s \sim 0.45, 0.75$ in Fig. 2), but still be sensitive to most galaxies and QSOs. Nearly all QSOs with redshifts below ~ 0.5 , selected at other wavelengths, have $J-K_s > 1.2$ (Francis et al. 2000; Barkhouse & Hall 2001; Cutri et al. 2002). At higher redshifts, the near-IR flux excess (Sanders et al. 1989) is shifted out of the K_s band, causing the average $J-K_s$ color of known AGNs to become bluer, but even at these higher redshifts, at least 10% of AGNs have $J-K_s > 1.2$.

The color cut eliminates some galaxies from our sample. The median $J-K_s$ color of galaxies in the 2MASS Extended Source Catalog (XSC) is ~ 1.1 . The mean color of galaxies shifts rapidly to the red with increasing redshift due to k -corrections though. At the magnitude limit of the 2MASS Point Source Catalogue (PSC; our input catalog), most galaxies will be unresolved and will lie at redshifts well above 0.1 where the median galaxy color is redder than $J-K_s = 1.2$. We estimate our incompleteness to galaxies by counting the number of 2MASS XSC sources with $J-K_s < 1.2$ in our survey areas and by cross-correlating the SDSS Early Release

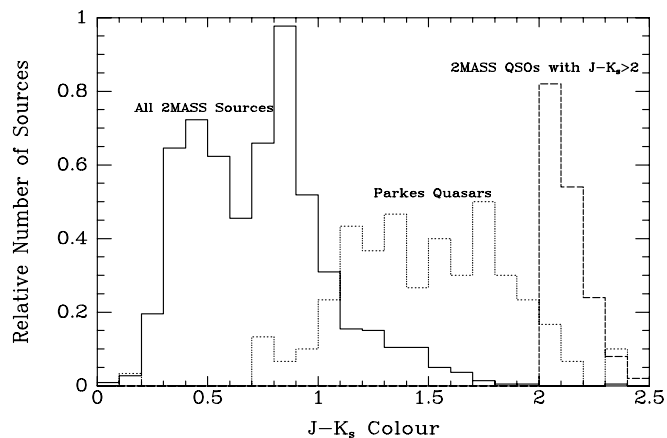


FIG. 2.—Distribution of $J-K_s$ colors for high galactic latitude 2MASS sources (solid line), type 1 AGNs selected as having $J-K_s > 2$ (dashed line, Cutri et al.), and radio-selected quasars from the Parkes Half-Jansky Flat Spectrum sample (dotted line, Francis et al. 2000).

galaxy catalog with the 2MASS PSC: fewer than 23% of galaxies would fail to meet our color cut. The missing galaxies will be predominantly at redshifts less than 0.1 and resolved by 2MASS.

The bias of our survey toward low redshift AGN does limit our ability to find dusty QSOs. The luminosity of most QSOs found in the local universe is only a little greater than that of their host galaxies. Even small amounts of dust extinction will thus reduce the AGN light below the host galaxy light, causing the source to be classified as a type 2 AGN rather than a dusty type I AGN. Spectacularly reddened type 1 AGNs should thus only be found in high-redshift, high-luminosity samples, such as that of Gregg et al. (2002).

Our target selection, observations, and data reduction are described in § 2, and the spectral classification of our sources in § 3. Our results are presented in § 4 and discussed in § 5. Finally, conclusions are drawn in § 6

2. OBSERVATIONS AND REDUCTION

2.1. Target Selection

Targets were selected from the 2MASS Point Source Catalog. Note that this catalog includes extended sources. All cataloged sources with $J-K_s > 1.2$ and detections in all three bands were potential targets, regardless of optical magnitude or morphology. No attempt was made to exclude previously observed sources.

We observed spectra of sources in four fields. Each field was circular and 1° in radius. The fields were centered at 09:44+00:00, 12:44+00:00, 13:00–25:00, and 14:15–26:00 (J2000.0). The first two fields were chosen to overlap with the imaging data from the Early Data Release of SDSS (Stoughton et al. 2002). All fields lie at Galactic latitudes greater than 30° .

Observations were carried out with the Two Degree Field (2dF) spectrograph on the Anglo-Australian Telescope (AAT; Lewis et al. 2002). This spectrograph has 400 fibers, spread over a circular field of radius 1° , located at the prime focus of the AAT. Each fiber has a projected diameter of $2''$ on the sky. A small number of fibers were set aside to measure the sky spectrum. The remaining fibers were allocated to targets using the *configure* program (Lewis et al. 2002). The program was set to allocate fibers to the brightest K_s -band sources first and

then progressively to the fainter ones. We were able to allocate fibers to all 69 sources with $K_s < 14.0$, 677 of the 873 sources with $14.0 < K_s < 15.0$, but only 780 of the 1407 sources with $15.0 < K_s < 15.5$. The incompleteness in the $14.0 < K_s < 15.0$ range is mostly due to fiber positioning constraints, while the incompleteness at fainter magnitudes is due to the limited number of fibers. The incompleteness that this introduces should be random in every parameter except K -band magnitude. The magnitude and color distribution of the sources for which we obtained spectra are shown in Figure 3.

2.2. Observations and Reduction

Spectra were taken of sources in our four fields on the nights of 2002 March 5–7. Conditions were partially cloudy at times, and the seeing was typically around $1''.8$. Each field was observed with two different fiber configurations: one for the brightest ~ 30 sources and the other for the remaining ~ 350 . This technique was chosen to minimize scattered light problems. Exposure times were 600–900 s for the bright object configurations and 10,036–10,800 s for the faint object configurations. Bright sources in the 1415–2600 field were not observed, due to cloud. The 300R and 316R gratings were used in the two spectrographs, giving a spectral resolution of 10 \AA and a wavelength coverage of 4500–8500 \AA .

The data were reduced using the 2DFDR software (Lewis et al. 2002), using standard settings. All galaxy spectra were averaged (in the observed frame) to provide a template atmospheric absorption spectrum. The individual spectra were divided through by this template, which did a reasonably good job of correcting for these absorption bands. The spectra are not of spectrophotometric quality.

Spectra were obtained for a total of 1526 sources. Fifty-nine of these spectra were of such poor quality that regardless of the nature of the source, no spectral classification was possible. Figure 3 shows that the unusable quality spectra are predominantly those of the brighter sources. This was mainly caused by poor weather: the bright objects in one of the four fields were never observed, while in two other fields they were observed through significant cloud cover. Observations of the fainter sources were not as badly affected.

3. CLASSIFICATION

An initial classification was attempted for all spectra using the software developed for the 2dF Galaxy Redshift Survey

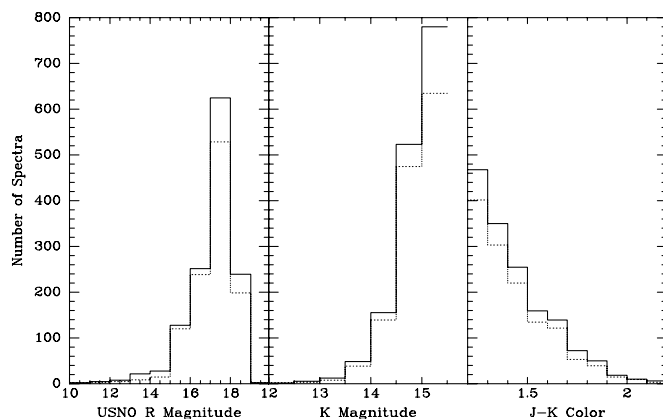


FIG. 3.—Number of spectra observed (solid line) and the number for which we secured a reliable spectral identification, either manually or automatically (dotted line), as a function of R magnitude (taken from the USNO-A catalog), K_s magnitude, and $J-K_s$ color.

TABLE 1
WAVELENGTH REGIONS USED IN EMISSION-LINE MEASUREMENTS

Line	Continuum Integration Limits (nm)	Line Integration Limits (nm)
H β	474.0–484.0, 488.0–494.0	484.5–488.0
[O III]	488.0–494.0, 503.0–510.0	499.0–502.5
H α	640.0–652.0, 663.0–670.0	655.0–657.2
N II	640.0–652.0, 663.0–670.0	657.2–659.4
[S II]	663.0–670.0, 674.5–684.5	670.0–674.5

(Colless et al. 2001). This software is optimized for measuring galaxy redshifts from 2dF spectra of comparable quality to our own and uses template fitting, line fitting, and cross-correlation techniques to classify spectra and to measure redshifts. All classifications were checked manually and assigned a quality flag. The program produced high-quality classifications and (where relevant) redshifts for around 80% of our spectra. It showed excellent performance for galaxies in our sample but was less reliable for broad-line AGNs and stars. The remaining spectra were checked by eye, and in many cases secure identifications could be made interactively.

3.1. Emission-Line Diagnostics

Galaxies showing H α and/or H β emission lines with velocity widths (FWHM height) greater than 1000 km s⁻¹ were classified as type 1 AGNs. Emission-line ratios were measured automatically for the remaining galaxies, by interpolating a straight-line continuum under them and summing the flux above this continuum. Wavelength regions used to define the continuum and over which line fluxes were summed are shown in Table 1. The effect of the underlying stellar absorption lines was corrected for by measuring the mean absorption-line equivalent width of the lineless galaxies in the sample and adding this to the measured emission-line equivalent widths. This assumes that the underlying stellar continua of emission-line and non-emission-line galaxies are the same, which will only be true to first approximation. These corrections are small: 0.05 nm for H α , 0.18 nm for H β , 0.15 nm for [O III], -0.07 nm for N II, and 0.005 nm for S II. To check that these corrections did not significantly affect our results, we repeated our classification without making them. This did not alter the classification of any of our galaxies,

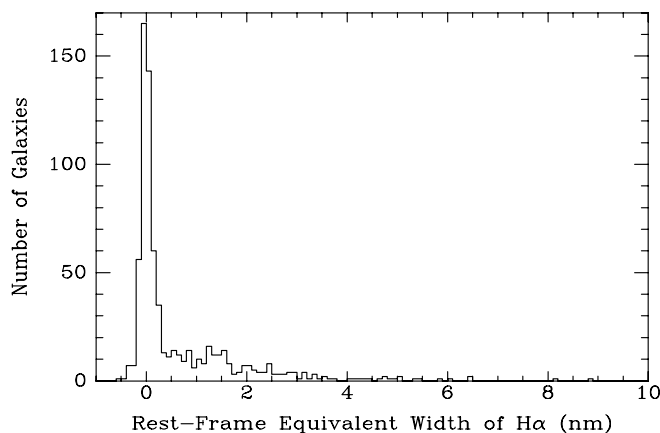


FIG. 4.—Histogram of measured rest-frame H α emission-line equivalent widths for all galaxies with acceptable quality spectra at the relevant wavelengths.

principally because the most affected sources were Seyfert 2 galaxies with very weak H β emission, and these lie a long way from the selection boundary. All line measurements were checked by eye and awarded a quality flag: 6% of spectra were too poor at the relevant wavelength to obtain a good measurement of H α . This was usually caused by H α falling on a strong sky line or atmospheric absorption band.

We estimate our equivalent width limit by looking at the dispersion in H α equivalent width measurements in galaxies with no detectable line emission (Fig. 4). We estimate that we are sensitive to all galaxies with rest-frame H α equivalent widths of greater than 0.4 nm. This excludes the 6% of galaxy spectra which were too poor at the relevant wavelength.

All galaxies with adequate quality data in all emission lines were classified using the diagnostic diagrams of Kewley et al. (2001). The results are shown in Figure 5. The galaxies split cleanly between AGN and starbursts. The AGNs have the line ratios of Seyfert 2 galaxies and not of LINERs (low-ionization nuclear emission-line regions). The 23 sources lying above both classification lines were classified as type 2 AGNs, and the 34 lying below as starburst galaxies. One source lay above one line and below the other: we classified it as an unknown emission-line galaxy.

Unfortunately, while many galaxies had good-quality data for the lines near H α (N II and [S II]), the shorter wavelength lines (H β and [O III]) were often too weak for us to be able to calculate their position along the y -axis of Figure 5. We note, however, a reasonably strong correlation between the x - and y -axes in the classification plots. If this correlation holds for the galaxies with weaker short wavelength lines, we can use it to tentatively classify at least

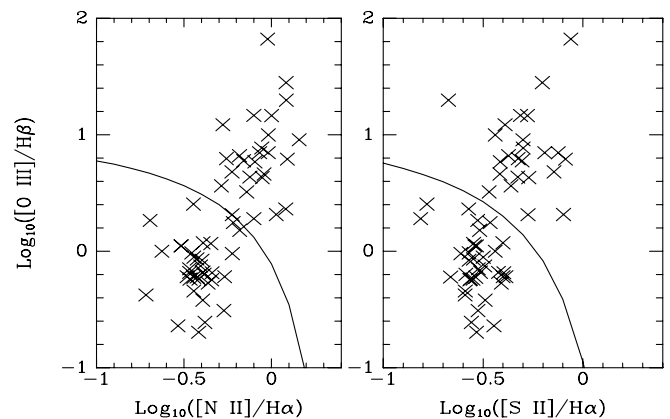


FIG. 5.—Line ratios of all galaxies with adequate quality data. The solid line is the theoretical classification boundary from Kewley et al. (2001). Sources lying above the boundary have emission lines excited by an AGN, while those below the boundary have lines excited by massive stars. One sigma error bars are typically ~ 0.1 in the log.

TABLE 2
SOURCE CLASSIFICATIONS AS A FUNCTION OF $J-K$ COLOR

$J-K_s$	Number of Classified Sources	Stars (%)	Galaxies (%)	Type 1 AGNs (%)	Type 2 AGNs (%)
Data in this paper:					
1.2–1.4.....	707	33	67	0.3	1.7
1.4–1.6.....	357	19	81	1.4	2.5
1.6–1.8.....	174	15	85	1.7	1.7
>1.8.....	66	9	91	6.0	0.0
Data from Cutri et al. (2002):					
>2.0.....	664	1	99	58	15

some of these sources. All otherwise unclassified emission-line galaxies with $\log(N\text{II}/H\alpha) > -0.2$ and $\log([\text{SII}]/H\alpha) > -0.35$ were classified as probable AGNs, while sources with $\log(N\text{II}/H\alpha) < -0.3$ and $\log([\text{SII}]/H\alpha) < -0.4$ were classified as probable starbursts. This yielded another 12 probable Seyfert 2 galaxies and 65 probable starburst galaxies. All other galaxies with $H\alpha$ equivalent widths greater than 0.4 nm were classified as unknown emission-line galaxies.

3.2. SDSS Data

We extracted data from the SDSS Early Data Release for the 739 of our targets lying within its region of coverage. For all but two of these sources, a SDSS cataloged source was found within $1''6$ of the 2MASS position. The median positional offset between the 2MASS and SDSS coordinates was $0''269$.

Two 2MASS sources did not have SDSS cataloged sources within $5''$ of the 2MASS position: 2MASS 0943007–000955 (an M dwarf star) and 2MASS 0946501+002050 (a galaxy at redshift 0.1414). As we obtained good spectra of both sources, using the $2''0$ diameter 2dF fibers centered at the 2MASS coordinates, the error must not lie in the 2MASS catalog.

All the 477 sources we classified as galaxies (on the basis of their spectra) were classified as extended sources by SDSS, while 147/156 stars were classified as point sources. Of the 68 sources with SDSS data that we were unable to classify based on their spectra, 54 (80%) were classified by SDSS as extended sources. A visual inspection of their spectra confirms

that most are probably galaxies without strong emission or absorption lines at wavelengths with good data.

4. RESULTS

We obtained 1526 spectra, of which 1467 were of usable quality. We were able to obtain secure classifications for 1298 of these spectra (88% completeness). As noted in § 3.2, the remaining unclassified sources are predominantly galaxies without strong absorption or emission lines at wavelengths for which we have good data. If any of these unclassified sources with usable quality spectra were AGNs with $H\alpha$ equivalent widths of greater than 0.4 nm, we would have detected their emission lines. The unclassified sources are concentrated in the fields observed through cloud: our successful classification rate is much higher in the fields observed in clear weather.

Three hundred thirty (25%) of the classified objects are stars. Around 20% are late K dwarfs, and the remainder are M dwarfs. The stars with SDSS data have a median $R = 19.22$. The fractions of objects with various classifications as a function of $J-K_s$ color are shown in Table 2.

The remaining 968 sources (75%) are galaxies of various types. Fourteen have broad emission lines and are hence type 1 AGNs (Table 3). Twenty-three are definite type 2 AGNs (Seyfert 2 galaxies), while another 12 are probable type 2 AGNs (as described in § 3.1). The type 2 AGNs are listed in Table 4. There are 106 galaxies whose line ratios make them definite or probable starburst galaxies, and a further 71 galaxies with $H\alpha$ rest-frame equivalent widths greater than

TABLE 3
TYPE 1 AGNs

NAME	POSITION (J2000.0)		R	K_s	$J-K_s$	REDSHIFT	PREVIOUS NAME
	R.A.	Decl.					
2MASS 09403186–0028433	09 40 31.86	–00 28 43.3	18.2	15.38	1.39	0.153	
2MASS 09441580+0011015	09 44 15.80	+00 11 01.5	17.2	14.61	1.51	0.128	SDSS J094415.78+001101.2
2MASS 09452492+0041448	09 45 24.92	+00 41 44.8	17.8	15.04	1.65	0.200	
2MASS 09460212+0035186	09 46 02.12	+00 35 18.6	18.1	14.85	1.73	0.649	SDSS J094602.11+003518.7
2MASS 12420264+0012191	12 42 02.64	+00 12 29.1	16.9	14.63	1.46	1.216	LBQS 1239+0028
2MASS 12442311+0027160	12 44 23.11	+00 27:16.0	17.8	15.02	1.49	0.165	SDSS J124423.07+002715.9
2MASS 12452459–0009379	12 45 24.59	–00 09 37.9	17.6	15.42	1.22	2.077	LBQS 1242+0006
2MASS 12461313–0042330	12 46 13.13	–00 42 33.0	16.7	14.46	1.49	0.649	LBQS 1243–0026
2MASS 13025113–2428552	13 02 51.13	–24 28 55.2	17.5	14.50	2.17	0.246	
2MASS 13031854–2435071	13 03 18.54	–24 35 01.7	17.4	14.69	1.84	2.255	HB 1300–243
2MASS 14161423–2607468	14 16 14.23	–26 07 46.8	17.5	14.25	1.70	0.220	
2MASS 14165581–2524134	14 16 55.81	–25 24 13.4	15.3	12.73	1.82	0.236	CTS 0025
2MASS 14180763–2548430	14 18 07.63	–25 48 43.0	16.8	14.73	2.02	0.494	
2MASS 14183782–2540138	14 18 37.82	–25 40 13.8	16.8	14.55	1.48	0.155	

NOTE.—Units of right ascension are hours, minutes, and seconds, and units of declination are degrees, arcminutes, and arcseconds.

TABLE 4
TYPE 2 AGNs

NAME	POSITION (J2000.0)		R	K_s	$J-K_s$	REDSHIFT	PREVIOUS NAME
	R.A.	Decl.					
Definite Seyfert 2 Galaxies							
2MASS 09444446+0035446	09 44 44.46	+00 35 44.6	17.9	15.15	1.52	0.1659	
2MASS 09412757-0020337	09 41 27.57	-00 20 33.7	16.2	15.31	1.21	0.1487	
2MASS 09443759+0034107	09 44 37.59	+00 34 10.7	17.5	14.75	1.52	0.1447	
2MASS 09410612-0028238	09 41 06.12	-00 28 23.8	16.4	14.81	1.47	0.1481	
2MASS 09472633-0005562	09 47 26.33	-00 05 56.2	17.4	14.96	1.47	0.1260	
2MASS 09415313+0009185	09 41 53.13	+00 09 18.5	16.5	14.13	1.75	0.1221	
2MASS 09422430-0000051	09 42 24.30	-00 00 05.1	16.1	14.16	1.80	0.1465	
2MASS 09425917+0031414	09 42 59.17	+00 31 41.4	16.3	14.36	1.39	0.0633	
2MASS 09430377+0008076	09 43 03.77	+00 08 07.6	17.0	14.93	1.33	0.1240	
2MASS 09452964-0021547	09 45 29.64	-00 21 54.7	13.2	14.00	1.24	0.0515	
2MASS 09451196-0007119	09 45 11.96	-00 07 11.9	12.4	13.64	1.37	0.0306	
2MASS 09441489+0018082	09 44 14.89	+00 18 08.2	17.1	14.75	1.47	0.1223	
2MASS 09443030+0045287	09 44 30.30	+00 45 28.7	17.0	14.88	1.32	0.1237	
2MASS 12432177+0015370	12 43 21.77	+00 15 37.0	17.1	14.86	1.38	0.1433	
2MASS 13031198-2447024	13 03 11.98	-24 47 02.4	17.8	15.22	1.31	0.1252	
2MASS 12593796-2523148	12 59 37.96	-25 23 14.8	15.6	13.87	1.50	0.0728	
2MASS 12595227-2516420	12 59 52.27	-25 16 42.0	12.8	13.01	1.36	0.0486	
2MASS 14143610-2546458	14 14 36.10	-25 46 45.8	16.6	15.27	1.55	0.1653	
2MASS 14132413-2615549	14 13 24.13	-26 15 54.9	16.0	14.54	1.72	0.1717	
2MASS 14140715-2528597	14 14 07.15	-25 28 59.7	16.2	14.66	1.33	0.1695	
2MASS 14143799-2520079	14 14 37.99	-25 20 07.9	17.2	14.85	1.35	0.1391	
2MASS 14154583-2518245	14 15 45.83	25 18 24.5	16.5	14.50	1.53	0.0750	
2MASS 14155435-2557332	14 15 54.35	-25 57 33.2	16.8	14.73	1.33	0.1681	
2MASS 14155854-2544131	14 15 58.54	-25 44 13.1	16.2	14.44	1.48	0.1697	
Probable Seyfert 2 Galaxies							
2MASS 09430751-0002492	09 43 07.51	-00 02 49.2	17.6	15.37	1.33	0.1247	
2MASS 09452796+0051041	09 45 27.96	+00 51 04.1	16.1	14.52	1.32	0.1431	
2MASS 12445756-0016176	12 44 57.56	-00 16 17.6	16.8	14.50	1.30	0.1186	
2MASS 12451295-0040566	12 45 12.95	-00 40 56.6	15.8	14.49	1.28	0.1043	
2MASS 12452522-0046579	12 45 25.22	-00 46 57.9	15.7	14.85	1.45	0.0806	
2MASS 12595666-2439065	12 59 56.66	-24 39 06.5	17.4	15.24	1.23	0.1053	
2MASS 13015692-2533499	13 01 56.92	-25 33 49.9	17.7	15.12	1.55	0.1859	
2MASS 12583172-2508040	12 58 31.72	-25 08 04.0	16.9	15.27	1.28	0.1045	
2MASS 13005827-2423430	13 00 58.27	-24 23 43.0	15.3	14.27	1.24	0.0993	
2MASS 12591093-2446418	12 59 10.93	-24 46 41.8	15.3	13.63	1.73	0.1125	
2MASS 12594636-2535568	12 59 46.36	-25 35 56.8	12.9	13.66	1.49	0.0639	ARP 1257-251
2MASS 14175559-2538535	14 17 55.59	-25 38 53.5	17.4	14.84	1.47	0.1209	
2MASS 14143476-2522301	14 14 34.76	-25 22 30.1	17.3	14.79	1.64	0.1159	

TABLE 5
ALL GALAXIES WITH SECURE REDSHIFTS

POSITION (J2000.0)		REDSHIFT	QUALITY	CLASS	K_s	$J-K_s$	EQUIVALENT WIDTH (nm)				
R.A.....	Decl.						H α	H β	[O III]	N II	S II
09 40 06.62.....	-00 05 14.2	0.0629	5	Sb?	14.0	1.22	0.3	0.3	0.1
09 40 08.85.....	+00 15 07.8	0.0497	5	Gem	14.9	1.66	1.6	1.1	0.6
09 40 09.09.....	-00 14 41.1	0.1724	5	Gal	14.9	1.37
09 40 10.60.....	+00 13 12.6	0.0625	5	Sb?	13.8	1.40	0.5	0.3	0.1
09 40 11.62.....	-00 11 50.5	0.2045	5	Gal	15.4	1.36
09 40 14.73.....	-00 19 46.7	0.1256	5	Gal	15.0	1.28
09 40 19.15.....	+00 04 25.4	0.0904	5	Sb	14.9	1.72	5.0	0.7	0.4	1.7	2.0
09 40 20.75.....	+00 23 32.0	0.0162	4	Gal	15.0	1.27
09 40 28.31.....	+00 05 23.3	0.2468	5	Gal	15.2	1.45
09 40 31.86.....	-00 28 43.3	0.1542	5	Qso	15.4	1.39

NOTE.—Table 5 is presented in its entirety in the electronic edition of the *Astronomical Journal*. A portion is shown here for guidance regarding its form and content.

0.4 nm, but that we could not classify. The galaxies with SDSS data have a median $R = 17.65$. Redshifts and spectral classifications for all galaxies with adequate data are shown in Table 5.

SDSS classifies 91% of the galaxies without measurable $H\alpha$ emission as elliptical galaxies (i.e., a de Vaucouleurs profile fits significantly better than an exponential profile). For emission-line galaxies (excluding AGNs) the fraction is 50%. The redshift histograms are shown in Figure 6. The galaxies without emission lines are quite strongly clustered: the peak seen at redshift 0.14 is due to one such cluster. The emission-line galaxies lie at a lower mean redshift than those without emission lines. This is probably because the emission-line galaxies are late type, while those without emission lines are massive luminous early-type galaxies and hence seen to larger distances.

The type 2 AGNs have a redshift distribution indistinguishable from that of other emission-line galaxies in the survey (Fig. 7). Most type 1 AGNs also lie at low redshifts, but there is a tail to very high redshifts.

5. DISCUSSION

5.1. The QSO Sample

We find 12 type 1 AGNs with $1.2 < J - K_s < 2.0$. Allowing for our incomplete spectroscopy of the faintest sources, this implies a surface density of 1.7 ± 0.5 type 1 AGNs per square degree, down to our selection limits (three-band detection by 2MASS in J , H , and K). Many of our sources, however, are fainter than the nominal completeness limit of the 2MASS survey. We estimated this completeness limit for our fields by comparing our K_s -band galaxy counts against the compilation of Huang et al. (2001). Down to $K_s = 15$, our target list appear to be highly complete: the statistical error due to our small sample of AGNs is much greater than any error caused by sample incompleteness. At this limit, and correcting for the unobserved targets, we find 1.0 ± 0.3 type 1 AGNs per square degree.

Are we missing many AGNs with $J - K_s < 1.2$? Barkhouse & Hall (2001) showed that essentially all low-redshift ($z < 0.5$) AGNs discovered by other techniques have $J - K_s > 1.2$ and should hence have been found in our survey. At higher redshifts, however, most AGNs have bluer $J - K_s$ colors. This is probably a k -correction effect: most AGNs show a sharp

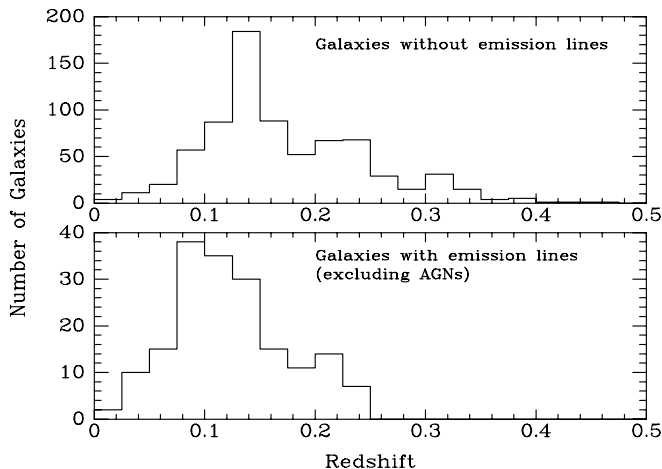


FIG. 6.—Redshift histogram for galaxies without $H\alpha$ emission (*top*) and with $H\alpha$ emission (*bottom*) down to our equivalent width threshold. Known or probable AGNs have been excluded.

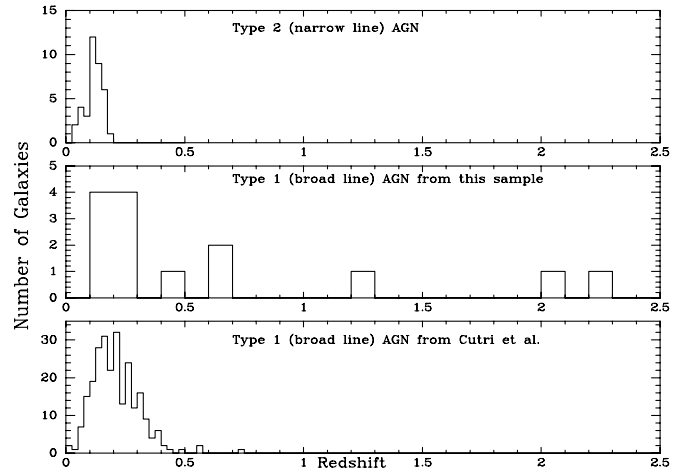


FIG. 7.—Redshift histogram for type 2 (narrow-line) AGNs (*top*), type 1 (broad-line) AGNs (*middle*) from this sample, and Type 1 AGNs with $J - K_s > 2$ from the sample of Cutri et al. (only southern hemisphere AGN with $K_s < 14.0$ and $R < 18$ shown).

rise in flux between rest-frame 1 and 2 μm , perhaps due to hot dust emission (e.g., Sanders et al. 1989), and at redshifts above 0.5, this is redshifted out of the K band. Only $\sim 10\%$ of high- z ($z > 0.5$) AGNs detected by other techniques have $J - K_s > 1.2$, except in the redshift range $2.2 < z < 2.5$, in which the $H\alpha$ emission line lies within the K band. This is consistent with our redshift distribution (Fig. 7).

Another way to test our completeness is to see whether we recovered previously known AGNs in our fields. The NASA Extragalactic Database (NED) lists 99 AGNs in our field, of which only nine meet our magnitude limits. Only one of the nine has $J - K_s < 1.2$. We recovered six of the remaining eight objects: we did not put fibers on the other two sources.

We can, therefore, place a lower limit on the surface density of type 1 AGNs of $1.0 \pm 0.3 \text{ deg}^{-2}$, down to $K = 15$. This matches the surface density of optically selected AGNs down to $B \sim 18.5$ (Meyer et al. 2001). Given that a typical quasar has $B - K \sim 3.5$ (Francis et al. 2000), this suggests that we may be seeing the same population sampled by optical surveys. This comparison should be treated with caution, however, as most optically selected QSOs down to $B = 18.5$ lie at redshifts to which we are largely insensitive, and most of our AGNs have such low luminosities that they would be discarded from most optical samples due to host galaxy contamination (§ 5.2).

5.2. Could These QSOs be Found by Conventional Techniques?

As Table 3 shows, only 57% of the type 1 AGNs, and none of the type 2 AGNs had been previously identified as AGNs. All five type 1 AGNs with redshifts above 0.5 had been previously identified.

In Figure 8, we compare the optical colors of our AGNs with the colors of field stars and galaxies. Only sources overlapping with the SDSS Early Data Release are shown. Our AGNs are clearly separated from the stellar locus. Half the type 1 AGNs are also well separated from the galactic locus, but the other half are not, and the type 2 AGNs also lie well within the galactic locus. This explains why so many of our sources were not previously identified: they are spatially resolved and have galaxy-like optical colors. Adding near-IR photometry does not help: their spectral energy distributions

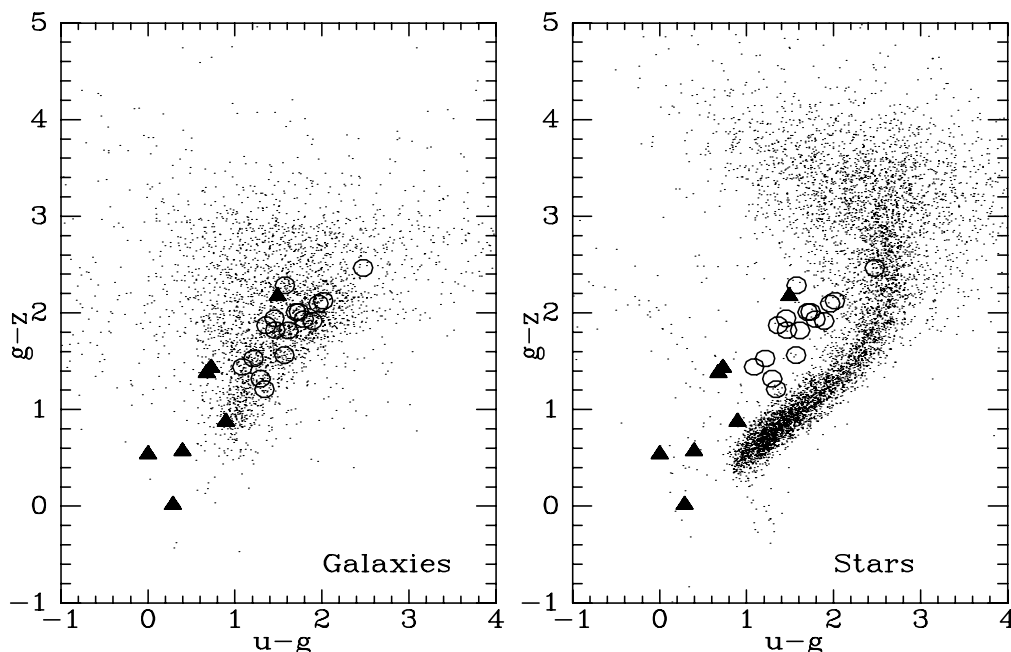


Fig. 8.—Optical colors of our type 1 (triangles) and type 2 (circles) AGNs, compared with all SDSS sources classified as galaxies (left) and stars (right)

are indistinguishable from those of inactive galaxies all the way from the U to the K_s band.

Why do the colors of so many of our sources resemble galaxies? The spectra of all AGNs with galaxy-like colors show strong stellar absorption lines, so their colors are probably dominated by the host galaxy and not by nuclear emission. Furthermore, Figure 9 shows that the K_s -band magnitudes of these AGNs are comparable to those of inactive galaxies at the same redshifts. We thus conclude that the host galaxy, rather than the nucleus, is dominating the observed continuum flux at all wavelengths.

While these AGNs would not be identified as such on the basis of their broadband colors, their strong broad $H\alpha$ emission lines would make them detectable in objective prism surveys, and large galaxy redshift surveys should contain thousands of them.

5.3. Dusty QSOs?

Is there a large population of dusty red QSOs? We are unable to determine whether our low-redshift AGNs are dust-reddened, since the host galaxies dominate their broadband colors, and since our observations are not spectrophotometric, we cannot determine the reddening by looking at line ratios. It is possible that their spectra are dominated by host galaxy light precisely because they are dusty. Alternatively, their nuclei could be intrinsically less luminous, or their host galaxies intrinsically more luminous than those of optically selected AGNs with the same K_s -band luminosities.

This leaves the small number of high-redshift QSOs. SDSS colors are available for four of these sources. All four are quite blue: their mean $g-K_s$ color is 2.86, which is very comparable to that seen in optically selected QSO samples (Francis et al. 2000). None are more than 0.7 mag redder than the mean in $g-K_s$, corresponding to $A_V = 0.8$ (for dust with an optical depth inversely proportional to wavelength).

We thus see no evidence for a population of dusty red QSOs. Our sample is, however, too small to place strong constraints. Let us define a red QSO as one with $g-K_s > 3.5$,

corresponding to $A_V > 0.8$. The fact that none of the four high- z QSOs with SDSS data meet this definition allows us to say with 95% confidence that no more than 50% of QSOs down to our magnitude limit are red. As shown in Figure 1, however, imposing even a K -band magnitude limit will suppress the numbers of red AGNs by a factor of ~ 5 . Our limit is thus a weak one: no more than 80% of QSOs can be red. This is quite consistent with the limits derived from radio surveys (Francis et al. 2001; Gregg et al. 2002).

5.4. The Fraction of Galaxies with Active Nuclei

What fraction of the galaxies in our sample contained active nuclei, and how does this compare to the fraction found in blue galaxy samples?

We are only sensitive to AGNs with $H\alpha$ rest-frame equivalent widths of greater than 0.4 nm, within our aperture (our fibers are 2'' in diameter, which for the median redshift of the sample [0.15] corresponds to a physical diameter of 5 kpc).

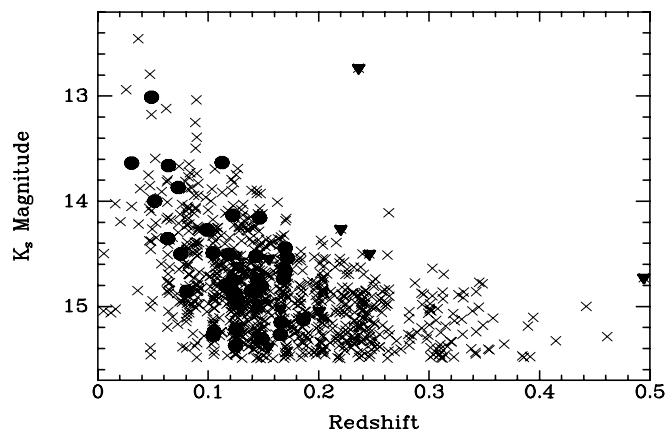


Fig. 9.—Redshifts and K_s -band magnitudes of all galaxies in our sample. type 1 AGNs are shown as filled triangles, and type 2 AGNs are shown as filled circles.

Ho et al. (1997) showed that we will miss most AGNs at this equivalent width limit, with our large aperture. In particular, we are mainly sensitive to Seyfert 2 galaxies and not to LINERs.

We obtained 1467 usable spectra, of which 330 were stars. Another 169 showed no significant emission or absorption features and are probably inactive galaxies. The remaining 968 are galaxies for which we were able to measure secure redshifts. Six percent of these galaxies had something wrong with their spectra at the wavelength of $H\alpha$. One hundred eighty-seven of the remaining galaxies had $H\alpha$ equivalent widths of greater than 0.4 nm. Of these, we were able to spectrally classify 116. We identified 14 type 1 AGNs and 35 type 2 definite or probable AGNs.

There are 71 galaxies with narrow $H\alpha$ lines above our selection threshold but with the signal-to-noise ratio too poor to allow classification. If we assume that these galaxies have the same relative proportions of type 2 AGNs and starburst galaxies as the 116 we could classify, then there are 58 type 2 AGNs in the sample.

The sample population in which we could have seen type 2 AGN activity is $968 + 169 = 1137$ galaxies. We thus estimate that $58/1137 = 5.1 \pm 0.9\%$ of galaxies in our sample were type 2 AGNs, down to our $H\alpha$ equivalent width limit (Poisson errors). If none of the unclassifiable emission-line galaxies were AGNs, which seems unlikely, the fraction would be $35/1137 = 3.1\%$. This gives a lower limit on the fraction. For type 1 AGNs, the fraction is $1.2 \pm 0.3\%$. Note also that our 35 definite or probable AGNs included several classified on the basis of their red emission lines only, as discussed in § 3.1.

How does this compare with the AGN fraction in blue-selected galaxy samples? Huchra & Burg (1992) only found Seyfert activity (of any type) in 1.3% of a sample of 2399 nearby galaxies. Unfortunately, they do not list their equivalent width threshold, so this number cannot be compared with our figure. Ho et al. (1997), however, find that nearly 50% of nearby blue-selected galaxies are AGNs, but they used nuclear spectra and were sensitive to much weaker lines than we are.

We defined a subsample of the Ho et al. (1997) sources that would have been classified as Seyfert galaxies by our criteria. Firstly, we had to correct for the different spectroscopic aperture. They typically measured the spectrum over a region of radius less than 200 pc, compared with our physical radii of ~ 2500 pc. To see how much difference this typically makes, we obtained archival CCD images of six Seyfert 2 galaxies from their sample, using the NED. We measured the broadband optical flux for each galaxy in a 200 pc aperture and a 2500 pc aperture. The fluxes in the larger apertures were greater by a factor of between 4 and 25.

Thus for one of their galaxies to have made it into our sample (if it were at the median redshift of our galaxies), it would need a nuclear $H\alpha$ equivalent width exceeding 1.6 nm (4×0.4 nm). Ho et al. (1997) also use slightly different diagnostics to identify AGNs, but this makes little difference to the final numbers.

We find that 1.5 ± 0.6 of their galaxies contained type 2 AGNs (meeting our selection criteria) and $1\% \pm 0.4\%$ contained type 1 AGNs. There is thus no significant difference in the fraction of type 1 AGNs, but we are finding a significantly higher fraction of type 2 AGNs.

Why do we find a higher fraction of galaxies with AGNs? Finding an AGN requires the presence of a black hole, a suitable

accretion rate of mass on to it, gas to be ionized by the nucleus, and a dust geometry that both allows this ionization to take place and allows us to see the resultant narrow line emission. Many of these factors could be different in an IR-selected sample. Since black hole masses are correlated with the stellar masses of the bulge (e.g., Magorrian et al. 1998), this may indicate that our sample of galaxies contain larger nuclear black holes than those found in blue-selected samples. On the other hand, blue galaxies typically have more gas and a higher star formation rate than red ones. Note also that our galaxies lie at higher redshifts than the Ho et al. (1997) sample and are on average more massive and luminous. We may simply be looking at a tendency for AGNs to be found in the most massive galaxies.

Could the difference simply be because the near-IR selected galaxies have less continuum flux at the wavelength of $H\alpha$? Our galaxies have a median $r-K_s = 2.77$, while blue-selected galaxies at similar magnitude limits have a median $r-K_s \sim 1.5$. Thus the younger stellar populations in the blue selected galaxies are increasing the continuum flux per unit stellar mass by a factor of ~ 3 . Even allowing for this, the fraction of Seyfert 2 galaxies in Ho et al. (1997) would only rise to $\sim 3\%$.

This result should be considered tentative. Secure line diagnostics are only available for around half of the Seyfert 2 population in our sample, and the comparison with the very different Ho et al. (1997) sample involves large corrections for the different AGN detection thresholds.

6. CONCLUSIONS

We have selected a small sample of AGNs in the near-IR, using the brute-force power of the 2dF spectrograph to minimize selection biases. Perhaps the most surprising thing about this sample is how similar it looks to conventional blue-selected AGN samples. While many of our type-1 AGNs would not have been found by optical techniques, in all cases this seems to be due to host galaxy contamination. Large galaxy surveys, such as the 2dF Galaxy Redshift Survey (Colless et al. 2001), are probably the best way to find such AGNs. Our sample of high-redshift QSOs was too small to usefully constrain the population of dusty red QSOs.

We tentatively conclude that the fraction of galaxies in our sample with AGN emission is greater than that found in the blue-selected galaxy sample of Ho et al. (1997). There are many possible reasons for this difference and discriminating between them will be difficult.

Finally, we can extrapolate from our data to estimate the number of AGNs in the 2MASS Point Source Catalog. There should be $\sim 50,000$ type 1 AGNs and $\sim 200,000$ type 2 AGNs that meet our selection criteria.

This publication makes use of data products from the Two Micron All Sky Survey, which is a joint project of the University of Massachusetts and the Infrared Processing and Analysis Center/California Institute of Technology, funded by the National Aeronautics and Space Administration and the National Science Foundation. Funding for the creation and distribution of the SDSS Archive has been provided by the Alfred P. Sloan Foundation, the Participating Institutions, the National Aeronautics and Space Administration, the National Science Foundation, the Department of Energy, the Japanese Monbukagakusho, and the Max Planck Society. The SDSS is

managed by the Astrophysical Research Consortium for the Participating Institutions. The Participating Institutions are the University of Chicago, Fermilab, the Institute for Advanced Study, the Japan Participation Group, Johns Hopkins University, Los Alamos National Laboratory, the Max-Planck-Institut für Astronomie, the Max-Planck-Institut für Astrophysik,

New Mexico State University, University of Pittsburgh, Princeton University, the US Naval Observatory, and the University of Washington. This research has made use of the NASA/IPAC Extragalactic Database, which is operated by the Jet Propulsion Laboratory, California Institute of Technology, under contract with NASA.

REFERENCES

- Alexander, D. M., Brandt, W. N., Hornschemeier, A. E., Garmire, G. P., Schneider, D. P., Bauer, F. E., & Griffiths, R. E. 2001, *AJ*, 122, 2156
- Baker, J. C., & Hunstead, R. W. 1995, *ApJ*, 452, L95
- Barkhouse, W. A., & Hall, P. B. 2001, *AJ*, 121, 2843
- Brotherton, M. S., Arav, N., Becker, R. H., Tran, H. D., Gregg, M. D., White, R. L., Laurent-Muehleisen, S. A., & Hack, W. 2001, *ApJ*, 546, 134
- Colless, M. M., et al. 2001, *MNRAS*, 328, 1039
- Courbin, F., Lidman, C., Frye, B. L., Magain, P., Broadhurst, T. J., Pahre, M. A., & Djorgovski, S. G. 1998, *ApJ*, 499, L119
- Croom, S. M., Warren, S. J., & Glazebrook, K. 2001, *MNRAS*, 328, 150
- Cutri, R. M., Nelson, B. O., Francis, P. J., & Smith, P. 2002, in *ASP Conf. Ser.* 284, *AGN Surveys*, ed. R. F. Green, E. Ye. Kachikian, & D. B. Sanders (San Francisco: ASP), 127
- Dopita, M. A., Heisler, C., Lumsden, S., & Bailey, J. 1998, *ApJ*, 498, 570
- Francis, P. J., Drake, C. L., Whiting, M. T., Drinkwater, M. J., & Webster, R. L. 2001, *Publ. Astron. Soc. Australia*, 18, 221
- Francis, P. J., Whiting, M. T., & Webster, R. L. 2000, *Publ. Astron. Soc. Australia*, 17, 56
- Gregg, M. D., Lacy, M., White, R. L., Glikman, E., Helfand, D., Becker, R. H., & Brotherton, M. S. 2002, *ApJ*, 564, 133
- Ho, L. C., Filippenko, A. V., & Sargent, W. L. W. 1997, *ApJS*, 112, 315
- Huang, J.-S., et al. 2001, *A&A*, 368, 787
- Huchra, J., & Burg, R. 1992, *ApJ*, 393, 90
- Kewley, L., Heisler, C., Dopita, M., & Lumsden, S. 2001, *ApJS*, 132, 37
- Lewis, I. J., et al. 2002, *MNRAS*, 333, 279
- Low, F. J., Cutri, R. M., Huchra, J. P., & Kleinmann, S. G. 1988, *ApJ*, 327, L41
- Magorrian, J., et al. 1998, *AJ*, 115, 2285
- Malhotra, S., Rhoads, J. E., & Turner, E. L. 1997, *MNRAS*, 288, 138
- Matute, I., et al. 2002, *MNRAS*, 332, L11
- McDowell, J. C., Elvis, M., Wilkes, B. J., Willner, S. P., Oey, M. S., Polomski, E., Bechtold, J., & Green, R. F. 1989, *ApJ*, 345, L13
- Meyer, M. J., Drinkwater, M. J., Phillips, S., & Couch, W. J. 2001, *MNRAS*, 324, 343
- Mushotzky, R. F., Cowie, L. L., Barger, A. J., & Arnaud, K. A. 2000, *Nature*, 404, 459
- Richards, G. T., et al. 2002, *AJ*, 123, 2945
- Sanders, D. B., Phinney, E. S., Neugebauer, G., Soifer, B. T., & Matthews, K. 1989, *ApJ*, 347, 29
- Schlegel, D. J., Finkbeiner, D. P., & Davis, M. 1998, *ApJ*, 500, 525
- Skrutskie, M. F., et al. 1997, in *The Impact of Large Scale Near-IR Sky Surveys*, ed. F. Garzon et al. (Dordrecht: Kluwer), 25
- Smith, P. S., Schmidt, G. D., Hines, D. C., Cutri, R. M., & Nelson, B. O. 2002, *ApJ*, 569, 23
- Stoughton, C., et al. 2002, *AJ*, 123, 485
- Warren, S. J., Hewett, P. C., & Foltz, C. B. 2000, *MNRAS*, 312, 827
- Webster, R. L., Francis, P. J., Peterson, B. A., Drinkwater, M. J., & Masci, F. J. 1995, *Nature*, 375, 469
- Whiting, M. T., Webster, R. L., & Francis, P. J. 2001, *MNRAS*, 323, 718
- Wilkes, B. J., Schmidt, G. D., Cutri, R. M., Ghosh, H., Hines, D. C., Nelson, B., & Smith, P. S. 2002, *ApJ*, 564, L65